Numerical simulation study on spin resonant depolarization due to spin–orbit coupling*

Lan Jie-Qin(蓝杰钦)† and Xu Hong-Liang(徐宏亮)‡

National Synchrotron Radiation Laboratory, University of Science and Technology of China, Hefei 230029, *China*

The spin polarization phenomenon in lepton circular accelerators had been known for many years. It provides a new approach for physicists to study the spin feature of fundamental particles and the dynamics of spin–orbit coupling, such as spin resonances. We use numerical simulation to study the features of spin under the modulation of orbital motion in an electron storage ring. The various cases of depolarization due to spin–orbit coupling through an emitting photon and misalignment of magnets in the ring are discussed.

Keywords: spin polarization and resonant depolarization, spin–orbit coupling, spin flip, numerical simulation

PACS: 45.10.–b, 21.10.Hw, 29.20.D– **DOI:** 10.1088/1674-1056/21/8/084501

1. Introduction

It was first predicted by Sokolov and Ternov[1] that an electron beam in circular accelerators can spontaneously become polarized antiparallel to the directing magnetic field through emitting spin-flip synchrotron radiation in the form of light quantum. For a beam that is nonpolarized initially, the build-up of polarization with time follows

$$P(t) = P_{\rm st}(1 - {\rm e}^{-t/\tau_{\rm st}}), \tag{1}$$

where $P_{\rm st} = 8/5\sqrt{3} \approx 0.9238$ is the so-called Sokolov–Ternov (ST) limit of equilibrium spin polarization and $\tau_{\rm st}$ is the relaxation time of the polarization process with a value normally ranging from several minutes to several hours in modern accelerators. That is good news for physicists since the high polarized beam saves the polarized source[2] required for exploring the spin structure of nucleons and the spin correlation in the basic of interaction. It is also extensively used in high-energy colliding experiments to test the standard electo-weak model[3] and used in storage rings for high accuracy calibrating beam energy.[4,5] Moreover, it gives a new approach to study about the feature and dynamics of spin, such as spin–orbit coupling resonances and resonance crossing in synchrotron.[6,7]

It is then noticed that in reality the attainable degree of equilibrium polarization is usually lower than the ST limit because there are many depolarization factors in a real synchrotron. Expression (1) is only valid for the situation where the ring is perfectly flat. Misalignment of magnets in the ring can cause distortion of the orbit and then electrons no longer pass through the center of the magnets. Any fields that are non-vertical will perturb and decrease the vertical polarization. Also, synchrotron radiation is known not only as the impetus of polarization but also the main source of depolarization. A particle that emits a photon would receive a recoil, which perturbs its subsequent orbital motion. The spin is then disturbed by the field that modulated by the orbital motion. This is the spin–orbit coupling course that causes spin diffusion. Spin–orbit coupling research is a hot topic in many fields.[8,9] In a storage ring when the tune (oscillation frequency in unit of the revolution frequency) of orbital motion modulation is in phase with the tune (precession frequency in units of revolution frequency) of the spin precession around the vertical field, the spin–orbit coupling attains considerable strength and the polarization of the beam is destroyed. Since the average spin tune is energy related as

$$\nu = a\gamma = \frac{E[{\rm MeV}]}{440.6486[{\rm MeV}]}, \tag{2}$$

where a, γ, and E are the magnetic moment anomaly, Lorentz factor, and energy of electron, respectively, one hopes to obtain the spin resonance spectrum versus beam energy so as to operate the machine at an

*Project supported by the National Natural Science Foundation of China (Grant No. 10875118).

†Corresponding author. E-mail: lanjq@mail.ustc.edu.cn

‡Corresponding author. E-mail: hlxu@ustc.edu.cn

© 2012 Chinese Physical Society and IOP Publishing Ltd

energy away from spin resonances or find a way to preserve polarization when spin resonances are encountered. For this reason, an effective numerical simulation may provide assistance. Researchers have tried to give an expression for estimating equilibrium polarization based on a given structure of a circular accelerator, e.g., a lattice. The most used expression is the Derbenev–Kondratenko–Mane (DKM) formula.[10,11] Estimation of the attainable equilibrium polarization between the balance of radiative polarization and radiative depolarization can be realized by numerically evaluating the formula. In addition, knowledge about the spin–orbit coupling resonance can help us to utilize the resonance spectrum for other physics research.

This paper is organized as follows. In Section 2 we begin with looking back at the basic theory of electron spin resonance. Then in Section 3 the more complicated spin resonant depolarization in view of spin–orbit coupling in a circular accelerator is elaborated. Following that, numerical simulation for estimating the attainable equilibrium polarization based on evolving the DKM formula is given in Section 4. Spin tracking results are shown for detailedly studying the spin behaviors away from resonance, at resonance, and near resonance. The result of the available resonant depolarization experiment is shown too. Section 5 includes our conclusions.

2. Theory of electron spin resonance

Suppose that there is a nonrelativistic spin-polarized electron along the y axis in the beginning, where there is a static magnetic field $\boldsymbol{B}_0 = -B_0\hat{y}$. There is also an alternating magnetic field existing orthogonal to this direction $\boldsymbol{B}_1(t) = B_1(\hat{x}\sin\omega t + \hat{z}\cos\omega t)$. Then we can start with the Hamiltonian of this system and solve the corresponding Schrödinger equation to obtain detailed information about the spin afterwards. The Hamiltonian of a nonrelativistic electron in this case can be written as (in S_y diagonalization representation)

$$H = -\frac{ge\boldsymbol{S}_{\rm op}}{2m_{\rm e}c}\cdot(\boldsymbol{B}_0+\boldsymbol{B}_1), \tag{3}$$

where $e<0$ is the elementary charge of an electron with spin $\boldsymbol{S}_{\rm op}$, $m_{\rm e}$ is the rest electron mass, g is the gyromagnetic ratio, and c is the velocity of light. Represented with the Pauli two-component formalism of the spinor and using cyclic permutation, the Hamiltonian is rewritten as

$$\begin{aligned} H &= -\frac{ge\hbar}{4m_{\rm e}c}\begin{pmatrix} -B_0 & B_1\,{\rm e}^{-{\rm i}\omega t} \\ B_1\,{\rm e}^{{\rm i}\omega t} & B_0 \end{pmatrix} \\ &= \frac{\hbar}{2}\begin{pmatrix} -\omega_0 & \omega_1\,{\rm e}^{-{\rm i}\omega t} \\ \omega_1\,{\rm e}^{{\rm i}\omega t} & \omega_0 \end{pmatrix}, \end{aligned} \tag{4}$$

where $\hbar$ is the reduced Planck constant, $\omega_0 = -(ge/2m_{\rm e}c)B_0$ and $\omega_1 = -(ge/2m_{\rm e}c)B_1$. If the frequency of alternating magnetic field satisfies $|\omega| = |\omega_0|$, using the initial condition that $|\psi;t=0\rangle = \left(\begin{smallmatrix}1\\0\end{smallmatrix}\right)$ we can obtain the spinor at $t>0$ as follows:

$$|\psi;t>0\rangle = \begin{pmatrix} \cos(\omega_1 t/2)\cdot\,{\rm e}^{{\rm i}(\omega_0/2)t} \\ -\sin(\omega_1 t/2)\cdot\,{\rm e}^{{\rm i}(\pi/2-\omega_0/2t)} \end{pmatrix}. \tag{5}$$

Then we know the spin motion will follow a rule like that: (i) when $t=\pi/\omega_1, 3\pi/\omega_1, 5\pi/\omega_1, \ldots$ the spin flips down; (ii) and when $t=2\pi/\omega_1, 4\pi/\omega_1, 6\pi/\omega_1, \ldots$ the spin flips up again. That is to say, the spin will flip back and forth unless the magnetic field is canceled. The strength of alternating magnetic field determines how fast the spin-flip will be. This phenomenon is well known as the electron spin resonance (ESR).[12]

3. Spin resonant depolarization due to spin–orbit coupling in circular accelerator

In a circular accelerator like a storage ring where there are a number of electrons cycling around the ring for a long time, there are also spin resonances. But the resonance phenomenon is now much more complicated since the spin motion of an electron is dominated and modulated by its orbital motion. The electron is now moving with relativistic velocity at nearly the speed of light. The motion of the spin vector defined in the rest frame of the particle is described by the Thomas-BMT equation[13,14]

$$\frac{{\rm d}\boldsymbol{S}}{{\rm d}t} = \boldsymbol{\Omega}_{\rm bmt}\times\boldsymbol{S}, \tag{6}$$

where

$$\begin{aligned} \boldsymbol{\Omega}_{\rm bmt} = -\frac{e}{m_{\rm e}c}\Bigg[&\left(a+\frac{1}{\gamma}\right)\boldsymbol{B} - \frac{a\gamma}{\gamma+1}\boldsymbol{\beta}\cdot\boldsymbol{B}\boldsymbol{\beta} \\ &- \left(a+\frac{1}{\gamma+1}\right)\boldsymbol{\beta}\times\boldsymbol{E}\Bigg] \end{aligned} \tag{7}$$

is the spin precession vector with $\boldsymbol{E}$ and $\boldsymbol{B}$ denoting the electromagnetic field seen by spin, $\boldsymbol{\beta}$ denoting relative velocity and other quantities have been stated before. It depends on the particle energy, the azimuth along the ring and the canonical coordinates of the particle in phase space $\boldsymbol{X} = (x, x', y, y', z, \delta)$, where x, y, and z are the displacements of particle away from design orbit in radial, vertical, and longitudinal directions, respectively, x' and y' are the corresponding conjugate momenta and $\delta = \Delta E/E_0$ is the relative energy deviation with respect to the designed energy.

For an ideal situation that the ring is perfectly flat and the electron cycles along the designed orbit, the spin simply precesses around the direction of directing field in dipoles and the spin–orbit coupling vanishes. In this case, the polarization of the beam can reach the ST limit of 92.38%. But the fact is that there are some unavoidable misalignments of magnets and also a lot of electrons execute an oscillating motion around the newly formed equilibrium closed orbit (beam central trajectory). The misalignment of quadrupole acts on electron like a normal quadrupole $\boldsymbol{B} = k(x\hat{y} + y\hat{x})$ adding a horizontal dipole $\boldsymbol{B} = kx_{\mathrm{e}}\hat{y}$ and a vertical dipole $\boldsymbol{B} = ky_{\mathrm{e}}\hat{x}$, where x_{e} and y_{e} are the misalignment of quadrupole about the designed center. The horizontal component $ky_{\mathrm{e}}\hat{x}$ will perturb spin motion from vertical precession. The dipole rolling also brings in a transverse radial field that perturbs vertical spin precession. Furthermore, the spin of an oscillating electron motivated by photon recoil will suffer a horizontal perturbation when it goes through a quadrupole with a vertical deviation away from the center of the magnet. These perturbations will add coherently and cause beam depolarization if the resonance condition below is fulfilled

$$\nu_d = nP \tag{8}$$

or

$$\nu_d = n + n_y\nu_y. \tag{9}$$

Here ν_d means resonance spin tune, P means the superperiod numbers of the ring (since there are a number of random errors in a real ring, P actually equals 1), ns' are integer and ν_y is the vertical orbital tune of oscillation of particle. The first one is called imperfection resonance since it is caused by an imperfect ring and closed orbit distortion. The second one is called intrinsic resonance since it is caused by the oscillation of a particle and this is intrinsic. We can see that, how the orbital motion is determines how the spin motion will be in a circular accelerator. We are able to understand the spin motion only if we have adequately knowledge about the orbital motion and the spin–orbit coupling.

For more general case, the spin resonance will occur whenever the spin tune equals the linear combination of orbital motion tunes[15]

$$\nu_d = n + n_x\nu_x + n_y\nu_y + n_z\nu_z, \tag{10}$$

where ν_x and ν_z are horizontal and synchrotron (i.e., longitudinal) tunes of orbital oscillation. The resonances involving a synchrotron tune are called synchrotron sideband resonances. They arise from phase modulation on spin caused by the synchrotron motion. The resonances involving horizontal tune are called coupling intrinsic resonances and are due to the linear betatron coupling between horizontal and vertical oscillation. The betatron coupling exists mainly due to skew quadrupoles and solenoids in the ring. The sum $(|n_x| + |n_y| + |n_z|)$ is called the order of the resonance and the resonances that $|n_x|+|n_y|+|n_z| \geqslant 2$ are called higher-order spin resonances. The higher-order spin resonances[16] are not easy to calculate and will not be discussed below. They originate from spin perturbation due to nonlinear magnetic multipoles in the ring and linear betatron coupling. An excellent review of nonlinear dynamics can be found in Ref. [17].

4. Studying the spin behavior under orbital modulation with numerical simulation

Now we begin to study the spin polarization and resonant depolarization by numerical simulation. The Hefei Light Source (HLS) at the National Synchrotron Radiation Laboratory (NSRL) is used as an example. First, we estimate the attainable equilibrium polarization based on evolving the DKM formula. Then spin tracking is used as an alternate means to observe the behaviors of a classical spin vector in various situations. Tracking gives us more intuitive information about spin under the orbital modulation. It is helpful for us to understand the spin resonances. At the end, the result of an available spin resonant depolarization experiment by observing counting rate of the beam is given.

4.1. Simulation of the equilibrium polarization with the DKM formula

The DKM formula[10,11] for estimating attainable equilibrium polarization is

$$P_{\rm dkm} = \frac{8}{5\sqrt{3}} \cdot \frac{\left\langle \frac{1}{|\rho|^3}\hat{b}\cdot\left(\hat{n}-\gamma\frac{\partial\hat{n}}{\partial\gamma}\right)\right\rangle}{\left\langle \frac{1}{|\rho|^3}\left[1-\frac{2}{9}(\hat{v}\cdot\hat{n})^2+\frac{11}{18}|\gamma\frac{\partial\hat{n}}{\partial\gamma}|^2\right]\right\rangle}, \quad (11)$$

which includes all the information of spin in the two quantities, spin quantization axis $\hat{n}$, and spin–orbit coupling vector $\gamma\partial\hat{n}/\partial\gamma$. Here ρ is the radius of the curvature of a particle in the field, $\hat{v}$ is the unit vector of speed, $\hat{b} = \hat{v}\times\hat{\dot{v}}/|\hat{v}\times\hat{\dot{v}}|$ and the angular brackets denote an average around the ring and over the phase space of particles. $\hat{n}$ reflects the information of steady spin direction while $\gamma\partial\hat{n}/\partial\gamma$ reflects the information of spin diffusion, i.e., depolarization. The depolarization information (resonance and off-resonance) caused by both the non-vertical field and photon recoil can be included only if $\hat{n}$ and $\gamma\partial\hat{n}/\partial\gamma$ are properly defined and known well enough. A proper evaluation of the formula can give a result that can exactly reflect the various kinds of resonances. Note here, that only longitudinal momentum recoil is considered. The effects of the transverse momentum recoils from photon emissions are smaller than longitudinal by a factor $1/\gamma$ and negligible for real accelerators.

There are many computer algorithms[18−20] available to evaluate the DKM formula. We use the SLIM formalism[18,21] here. The SLIM formalism uses a 3×3 spin transfer matrix attached to the trajectory closed orbit to study the spin on the beam center. The trajectory closed orbit must be known beforehand. The 3×3 spin transfer matrix can be obtained from expression (6). By multiplying all the spin transfer matrices along the trajectory closed orbit for one turn, one can obtain the one turn map (OTM) for spin. Then the spin closed orbit, i.e., the steady spin direction on this orbit can be derived by solving the eigenvector of the spin OTM with unit eigenvalue. When the steady spin direction is obtained, an orthogonal spin base can be established to analyse the spin motion off-axis. The status of a particle is now characterized as an 8×1 state vector $\boldsymbol{V}$ that employs 6 components (as the vector $\boldsymbol{X}$ stated before) to represent orbit state and 2 added components to represent spin state with respect to closed orbit. Then instantaneous point photon emission causes no change of the particle status except for its 6-th component. The change of state vector is $\Delta\boldsymbol{V} = (0,0,0,0,0,\delta E/E,0,0)^{\rm T}$ with δE denoting the energy loss due to photon emission and T denoting transposition of the matrix. This perturbation can be projected onto the eigenstates of the OTM for the particle status. The projection, giving the information of diffusion due to photon recoil, can be obtained by using the orthogonality of eigenstates. Then the spin diffusion due to photon recoil is considered by defining the spin–orbit coupling vector $\gamma\partial\hat{n}/\partial\gamma$ as

$$\hat{n}_{\rm f} - \hat{n}_{\rm i} = \frac{\delta E}{E}\left(\gamma\frac{\partial\hat{n}}{\partial\gamma}\right), \quad (12)$$

where $\hat{n}_{\rm i}$ and $\hat{n}_{\rm f}$ denote the steady spin direction before and after emitting a photon. It is characterized by the last two components of the state vector $\boldsymbol{V}$.

The simulation result of attainable equilibrium polarization at HLS is shown in Fig. 1. We can see there are many resonances in the energy range. The imperfection spin resonances are separated with an energy distance of about 440.6 MeV through expression (2). The intrinsic resonances are marked out in the figure too. It is clear that at some energies, e.g., 440.65 MeV, 551.95 MeV, and 881.28 MeV, the beam polarization is badly destroyed since the depolarization is strong there. At the location where the resonance is strong, the resonance width is wide. These resonances are usually harmful and cannot be ignored. Because the synchrotron tune here is too small, the sideband resonances overlap with the strong resonances and are undetectable at the side of the weak resonances. There are no skew quadrupoles or solenoids added here, so the coupling intrinsic resonances are weak and will not be discussed latter.

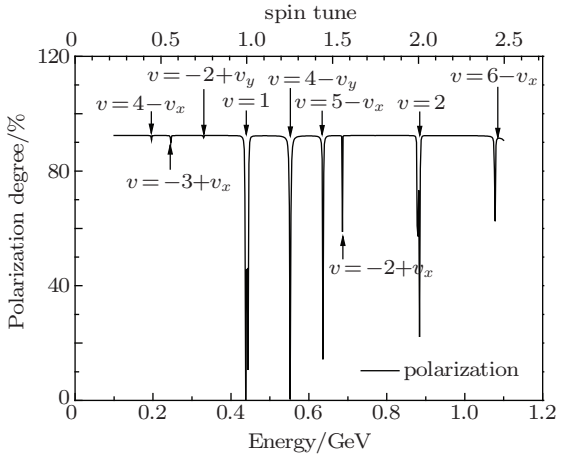


Fig. 1. Attainable equilibrium polarization versus beam energy.

4.2. Observation of classical spin trajectory by tracking

Alternately, we use the tracking method to investigate the behaviors of spin under the modulation of orbital motion. Spin tracking is more straightforward and intelligible. It can show us the concrete trajectory of spin either at resonance or away from resonance. For simplicity, we inspect the spin of a single electron with initial state $\hat{\boldsymbol{S}} = (0, 1, 0)$ and track it along the storage ring step by step and turn by turn. The tracking is based on expression (6). Tracking about the orbit and spin must proceed simultaneously since the spin is guided by the orbital motion.

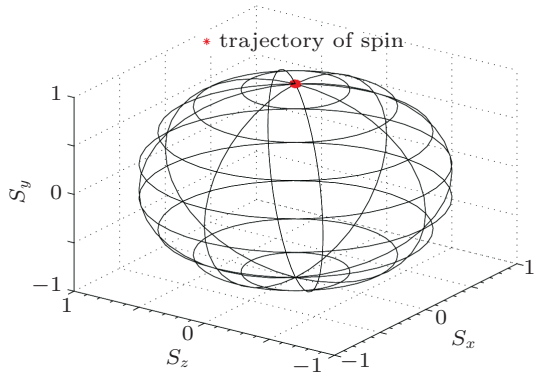


Fig. 2. (colour online) Trajectory of the unit vector of spin along the ring for 2000 turns when the spin resonance is away. $E = 800$ MeV, $\nu = 1.8155$. The initial condition is $\boldsymbol{X} = (0.0015, 0.00005, 0.00015, 0.00005, 0, 0)$ for an orbit that tracks out an ellipse of about 167-nm · rad emittance in horizontal phase space and 15-nm · rad emittance in vertical phase space, and $\hat{\boldsymbol{S}} = (0, 1, 0)$ for spin.

Three cases are investigated and the average features of spin motion around the ring are displayed in Figs. 2–4, respectively. Figure 2 shows the spin motion during the particle cycles around the ring for 2000 turns when the spin resonance is away ($E = 800$ MeV for normal operation of HLS). We can see that even the spin vector is now perturbed by the magnetic field modulated with orbital motion, but the perturbation is irregular and almost isotropic while the resonance is away. So the direction of spin integrally points vertically and the effective polarization is hardlyreduced. Then Fig. 3 shows the situation when the energy of an electron is deliberately appointed at an imperfect spin resonance ($E = 881.28$ MeV) while Fig. 4 shows the situation of intrinsic spin resonance ($E = 551.95$ MeV). From Figs. 3 and 4, we see obviously that the spin deviates from the vertical direction and flip-down. A small perturbation accumulates a big deviation of spin through resonance. For imperfection resonance, the spin flips down after tracking about 400 turns around the ring and flips up again for another 400 revolutions. For intrinsic resonance the spin flips down with about 2500 turns and flips back with another 2500 turns. The phenomenon of spin-flip resonance occurs just as Section 2 describes. The trajectory of spin spreads over the whole three-dimensional space sphere so the effective polarization around the ring is now vanishing.

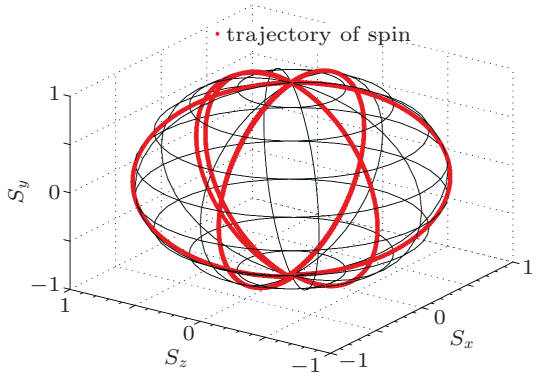


Fig. 3. (colour online) Trajectory of the unit vector of spin along the ring for 400 turns when the energy is at an imperfection spin resonance. $E = 881.28$ MeV, $\nu = 2$. The initial condition is $\boldsymbol{X} = (0, 0, 0, 0, 0, 0)$ for orbit and $\hat{\boldsymbol{S}} = (0, 1, 0)$ for spin. A set of random errors are added in the ring to generate a vertical distortion of closed orbit with a 2-mm RMS value.

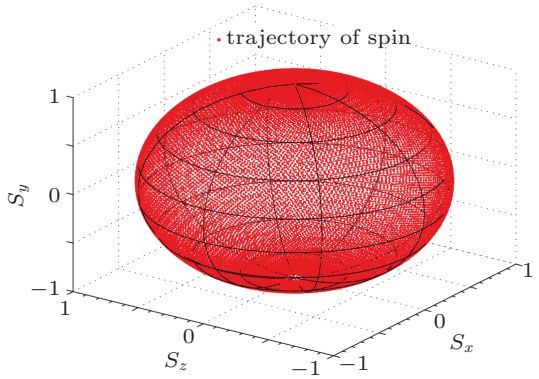


Fig. 4. (colour online) Trajectory of unit vector of spin along the ring for 2500 turns when the energy is at an intrinsic spin resonance. $E = 551.95$ MeV, $\nu = 4 - \nu_y = 1.2526$. The initial condition is $\boldsymbol{X} = (0.0015, 0.00005, 0.00015, 0.00005, 0, 0)$ for orbit and $\hat{\boldsymbol{S}} = (0, 1, 0)$ for spin.

To be more evident, we also inspect the spin motion with the fixed-point mapping method, i.e., observe the spin at a fixed azimuth of the ring for many turns and see the phase space average in this location. We can see from Fig. 5 that the trajectory of spin

flips down helically while the vertical spin precession is modulated coherently by the vertical oscillatory motion of orbit with tune $\nu_y = 2.7474$. The spin rambles all over the space, causing an averaging effect of trivial solution over the phase space. It is also interesting to study the spin behavior near resonance. To do so, we increase the energy with a step of 0.5 MeV from 880 MeV to 882.5 MeV and observe the spin trajectory near an imperfection resonance with a fixed-point mapping method. The exact resonance at 881.28 MeV is figured out too. Figure 6 shows that the closer the resonance is, the longer the spin trajectory will be. The effective polarization of this particle is then equivalent to spin points towards the center of the circular trace. When the spin tune is exactly at the resonance tune, spin walks through the maximal circle around the sphere and the effective vertical polarization is zero. When the spin tune is close to a resonance, the spin is partially flipped so there is still some effective vertical polarization preserved. This is determined by the resonance width. Thus we notice that in Fig. 1 some intrinsic resonances are not emerging, such as $v_d = v_y - 1$ and $v_d = 5 - v_y$. Tracking data about the resonance, taking $v_d = v_y - 1$ as an example, shows that this resonance is relatively weak and has a width of about 30 keV displayed in Fig. 7. These weak narrow resonances are usually hard to detect and are less harmful. But those strong resonances are relatively easy to detect in experiment.

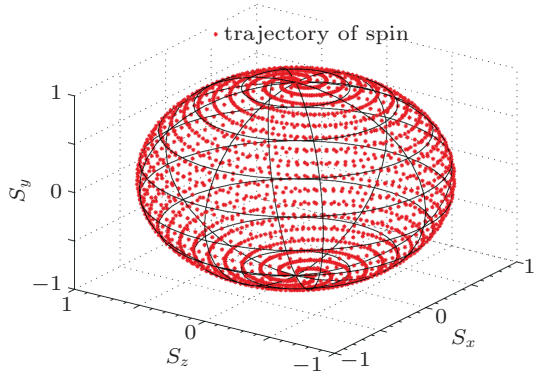


Fig. 5. (colour online) Trajectory of the unit vector of spin at an intrinsic resonance with the fixed-point mapping method. $E = 551.95$ MeV, $v = 1.2526$. The initial condition is $\boldsymbol{X} = (0.0015, 0.00005, 0.00015, 0.00005, 0, 0)$ for orbit and $\hat{\boldsymbol{S}} = (0, 1, 0)$ for spin.

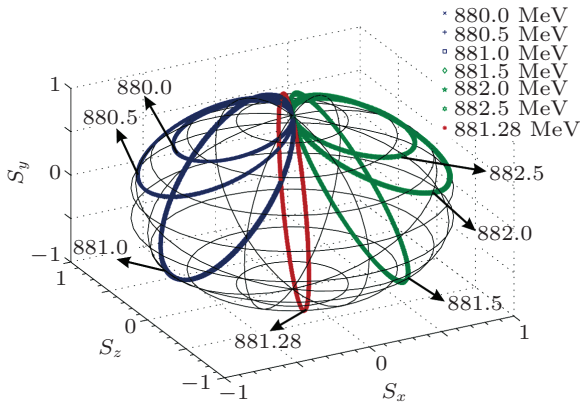


Fig. 6. (colour online) Investigating the behavior of spin with the fixed-point mapping method when the energy is close to an imperfection resonance. The initial condition is $\boldsymbol{X} = (0, 0, 0, 0, 0, 0)$ for orbit and $\hat{\boldsymbol{S}} = (0, 1, 0)$ for spin.

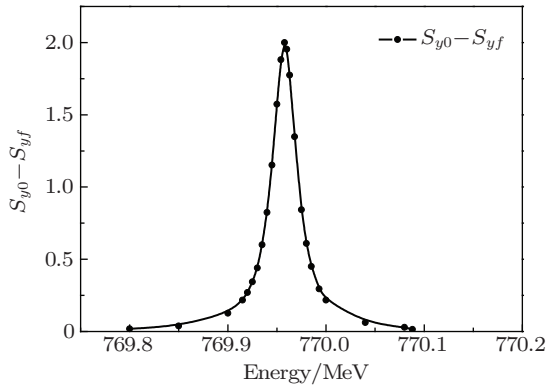


Fig. 7. Determining the width of relatively weak resonance by tracking. S_{y0} means the initial size of S_y, and S_{yf} means the maximum size of S_y after flipping.

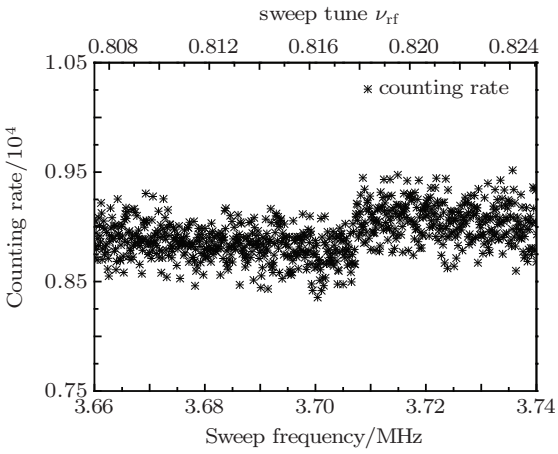


Fig. 8. Detection of the artificial spin resonant depolarization in experiment by observing counting rate of the beam.

In the actual operation, spin resonant depolarization can be indirectly detected by observing the beam counting rate. Since the counting rate is dependent on the spin polarization, a counting rate mutational signal can be seen when the resonance occurs. Instead of changing the energy, we artificially create spin resonance by adding a radial alternating magnetic field. When the frequency of the radial field fulfills $\nu = n + n_x\nu_x + n_y\nu_y + n_z\nu_z + \nu_{\rm rf}$, where $\nu_{\rm rf} = f_{\rm rf}/f_0$ is the frequency of radial field $f_{\rm rf}$ in unit of the revolution frequency f_0, the motion of spin resonantly

couples to the orbital motion. It is desirable to operate in the lowest mode, i.e., $\nu = n + \nu_{\rm rf}$. Here $n = 1$ is chosen. Figure 8 shows the situation of spin resonant depolarization when the frequency of the radial field sweeps around the spin tune. The spin resonance is observed at about 3.707 MHz of the sweep frequency.

5. Conclusion

We use numerical simulation with the SLIM formalism to estimate the equilibrium degree of polarization versus beam energy in a storage ring. This simulation is based on evolving the DKM formula, which is an elegant expression that includes various depolarizations due to spin–orbit coupling. The simulated result manifests that the resonance spectrum is abundant in a synchrotron. Straightforwardly, spin tracking about a single spin is implemented at some particle energies. Tracking step by step gives us a clearer image about spin under the modulation of orbital motion. The behaviors of spin away from resonance and at resonance are studied. Both spin vertical polarization preservation and spin-flip resonance are observed. Intrinsic and imperfection resonances are investigated in detail with the fixed-point mapping method to see the spin trajectory at resonances. Also, the behavior of spin near resonance is inspected and partial spin-flip is seen. The resonance width determines how much the spin can escape from flipping when it is near a resonance. Therefore, an example for obtaining the width of a narrow resonance that does not appear in Fig. 1 is shown. Finally, the result of an available spin resonant depolarization in the practical operation of the machine is given.

References

[1] Sokolov A A and Ternov I M 1964 *Sov. Phys. Dokl.* **8** 1203

[2] Gay T 1993 *Proceedings of the Workshop on Photocathodes for Polarized Electron Sources for Accelerators*, Stanford Linear Accelerator Center, Stanford, California September 8–10, 1993, p. 67

[3] Lynn B W 1988 *Polarization at LEP*, CERN, Geneva, Switzerland September, 1988, p. 24

[4] Arnaudon L, Dehning B, Grosse-Wiesmann P, Jacobsen R, Jonker M, Koutchouk J P, Miles J, Olsen R, Placidi M, Schmidt R, Wenninger J, Assmann R and Blondel A 1995 *Z. Phys.* C **66** 45

[5] Steier C, Byrd J and Kuske P 2000 *Proceedings of 7th European Particle Accelerator Conference*, Vienna, Austria, June 26–30, 2000, p. 1566

[6] Morozov V S, Chao A W, Krisch A D, Leonova M A, Raymond R S, Sivers D W, Wong V K, Garishvili A, Gebel R, Lehrach A, Lorentz B, Maier R, Prasuhn D, Stochhorst H, Welsch D, Hinterberger F and Kondratenko A M 2009 *Phys. Rev. Lett.* **102** 244801

[7] Leonova M A, Morozov V S, Krisch A D, Raymond R S, Sivers D W, Wong V K, Gebel R, Lehrach A, Lorentz B, Maier R, Prasuhn D, Schnase A, Stockhorst H, Hinterberger F and Ulbrich K 2006 *Phys. Rev. ST Accel. Beams* **9** 051001

[8] Yang J, Dong Q L, Jiang Z T and Zhang J 2011 *Acta Phys. Sin.* **60** 075202 (in Chinese)

[9] Yu Z Q, Xie Q and Xiao Q Q 2010 *Acta Phys. Sin.* **59** 925 (in Chinese)

[10] Derbenev Ya S and Kondratenko A M 1973 *Zh. Eksp. Teor. Fiz.* **64** 1918 [1973 *Sov. Phys.-JETP* **37** 968]

[11] Mane S R 1987 *Phys. Rev.* A **36** 105

[12] Wertz J E and Bolton J R 1972 *Electron Spin Resonance: Elementary Theory and Practical Applications* (New York: McGraw-Hill)

[13] Thomas L H 1927 *Phil. Mag.* **3** 1

[14] Bargmann V, Michel L and Telegdi V L 1959 *Phys. Rev. Lett.* **2** 435

[15] Lee S Y 1997 *Spin Dynamics and Snakes in Synchrotrons* (Singapore: World Scientific) p. 26

[16] Hoffstaetter G H and Vogt M 2004 *Phys. Rev.* E **70** 056501

[17] Chao A 1992 *Acta Phys. Sin.* (Overseas Edition) **1** 1013

[18] Chao A W 1981 *Nucl. Instrum. Method* **180** 29

[19] Mane S R 1987 *Phys. Rev.* A **36** 120

[20] Heinemann K and Hoffstätter G H 1996 *Phys. Rev.* E **54** 4240

[21] Chao A 2009 *Chin. Phys.* C **33** Suppl. II: 115